

# BPS AND NON-BPS DOMAIN WALLS IN SUPERSYMMETRIC QCD

A.V. SMILGA

*NORDITA, Blegdamsvej 17, DK-2100, Copenhagen Ø, Denmark <sup>a</sup>*

We study the spectrum of the domain walls interpolating between different chirally asymmetric vacua in supersymmetric QCD with the  $SU(N)$  gauge group and including  $N - 1$  pairs of chiral matter multiplets in fundamental and anti-fundamental representations. There are always “real walls” interpolating between the chirally symmetric and a chirally asymmetric vacua which are BPS saturated. For small enough masses, there are two different “complex” BPS wall solutions interpolating between different chirally asymmetric vacua and two types of “wall-some sphalerons”. At some  $m = m_*$ , two BPS branches join together and, in some interval  $m_* < m < m_{**}$ , BPS equations have no solutions, but there are solutions to the equations of motion describing a non-BPS domain wall and a sphaleron. For  $m > m_{**}$ , there are no complex wall solutions whatsoever.

## 1 Introduction

Supersymmetric QCD is the theory involving a gauge vector supermultiplet  $V$  and some number of chiral matter supermultiplets. The models of this class attracted attention of theorists since the beginning of the eighties and many interesting and non-trivial results concerning their non-perturbative dynamics have been obtained<sup>1</sup>. The dynamics depends in an essential way on the gauge group, the matter content, the masses of the matter fields and their Yukawa couplings.

The most simple in some sense variant of the model is based on the  $SU(N)$  gauge group and involves  $N - 1$  pairs of chiral matter supermultiplets  $S_{i\alpha}$ ,  $S_i'^\alpha$  in the fundamental and anti-fundamental representations of the gauge group with a common mass  $m$ . The lagrangian of the model reads

$$\mathcal{L} = \left( \frac{1}{4g^2} \text{Tr} \int d^2\theta W^2 + \text{H.c.} \right) + \sum_{i=1}^{N-1} \left[ \frac{1}{4} \int d^2\theta d^2\bar{\theta} \bar{S}_i e^V S_i + \frac{1}{4} \int d^2\theta d^2\bar{\theta} S_i' e^{-V} \bar{S}_i' - \frac{m}{2} \left( \int d^2\theta S_i' S_i + \text{H.c.} \right) \right], \quad (1)$$

---

<sup>a</sup>Permanent address: ITEP, B. Cheremushkinskaya 25, Moscow 117218, Russia

color and Lorentz indices are suppressed. In this case, the gauge symmetry is broken completely and the theory involves a discrete set of vacuum states. The presence of  $N$  chirally asymmetric states has been known for a long time. They are best seen in the weak coupling limit  $m \ll \Lambda_{SQCD}$  where the chirally asymmetric states involve large vacuum expectation values of the squark fields  $\langle s_i \rangle \gg \Lambda_{SQCD}$  and the low energy dynamics of the model is described in terms of the colorless composite fields  $\mathcal{M}_{ij} = 2S'_i S_j$ . The effective lagrangian presents a Wess–Zumino model with the superpotential

$$\mathcal{W} = -\frac{2}{3} \frac{\Lambda_{SQCD}^{2N+1}}{\det \mathcal{M}} - \frac{m}{2} \text{Tr } \mathcal{M} \quad (2)$$

The second term in Eq.(2) comes directly from the lagrangian (1) and the first term is generated dynamically by instantons. Assuming  $\mathcal{M}_{ij} = X^2 \delta_{ij}$  and solving the equation  $\partial \mathcal{W} / \partial \chi = 0$  ( $\chi$  is the scalar component of the superfield  $X$ ), we find  $N$  asymmetric vacua

$$\langle \chi \rangle_k = \left( \frac{4}{3} \frac{\Lambda_{SQCD}^{2N+1}}{m} \right)^{1/2N} e^{\pi i k / N} \equiv \rho_* e^{\pi i k / N} \quad (3)$$

(the vacua “k” and “k + N” have the same value of the moduli  $\langle \chi^2 \rangle_k$  and are physically equivalent). These vacua are characterized by a finite gluino condensate

$$\langle \text{Tr } \lambda^2 \rangle_k = 8\pi^2 m \langle \chi^2 \rangle_k \quad (4)$$

It was noted recently<sup>2</sup> that on top of (3) also a chirally symmetric vacuum with the zero value of the condensate exists. It cannot be detected in the framework of Eq.(2) which was derived *assuming* that the scalar v.e.v. and the gluino condensate are nonzero and large, but is clearly seen if writing down the effective lagrangian due to Taylor, Veneziano, and Yankielowicz (TVY)<sup>3</sup> involving also the composite field

$$\Phi^3 = \frac{3}{32\pi^2} \text{Tr } W^2 \quad (5)$$

The corresponding superpotential reads

$$\mathcal{W} = \frac{2}{3} \Phi^3 \left[ \ln \frac{\Phi^3 X^{2(N-1)}}{\Lambda_{SQCD}^{2N+1}} - 1 \right] - \frac{m}{2} N X^2 \quad (6)$$

Choosing kinetic term in the simplest possible form

$$\mathcal{L}_{\text{kin}} = \int d^4\theta (\bar{X}X + \bar{\Phi}\Phi), \quad (7)$$

the corresponding scalar potential is

$$U(\phi, \chi) = \left| \frac{\partial \mathcal{W}}{\partial \phi} \right|^2 + \left| \frac{\partial \mathcal{W}}{\partial \chi} \right|^2 = 4 \left| \phi^2 \ln \{ \phi^3 \chi^{2(N-1)} \} \right|^2 + (N-1)^2 \left| m\chi - \frac{4\phi^3}{3\chi} \right|^2 \quad (8)$$

(from now on we set  $\Lambda_{\text{SQCD}} \equiv 1$ ). The potential (8) has  $N+1$  degenerate minima. One of them is chirally symmetric:  $\phi = \chi = 0$ . There are also  $N$  chirally asymmetric vacua with  $\langle \chi \rangle_k$  given in Eq.(3) and

$$\langle \phi \rangle_k = \left( \frac{3m}{4} \right)^{(N-1)/(3N)} e^{-\frac{2i(N-1)\pi k}{3N}} \equiv R_* e^{-\frac{2i(N-1)\pi k}{3N}} \quad (9)$$

The presence of different degenerate physical vacua in the theory implies the existence of domain walls — static field configurations depending only on one spatial coordinate ( $z$ ) which interpolate between one of the vacua at  $z = -\infty$  and another one at  $z = \infty$  and minimizing the energy functional. As was shown in <sup>4</sup>, in many cases the energy density of these walls can be found exactly due to the fact that the walls present the BPS-saturated states.

The energy density of a BPS-saturated wall in SQCD with  $SU(N)$  gauge group satisfies a relation <sup>5</sup>

$$\epsilon = \frac{N}{8\pi^2} \left| \langle \text{Tr } \lambda^2 \rangle_\infty - \langle \text{Tr } \lambda^2 \rangle_{-\infty} \right| \quad (10)$$

where the subscript  $\pm\infty$  marks the values of the gluino condensate at spatial infinities.

Bearing Eqs. (10, 4) in mind, the energy densities of the BPS walls are

$$\epsilon_r = N \left( \frac{4m^{N-1}}{3} \right)^{1/N} \quad (11)$$

for the real walls interpolating between a chirally asymmetric and the chirally symmetric vacua (we call them “real” because the corresponding gauge field configurations are essentially real) and

$$\epsilon_c = 2\epsilon_r \sin \frac{\pi}{N} \quad (12)$$

for the complex walls interpolating between different chirally asymmetric vacua. The RHS of Eqs.(10-12) presents an absolute lower bound for the energy of *any* field configuration interpolating between different vacua.

The relation (10) is valid *assuming* that the wall exists and is BPS-saturated. However, whether such a BPS-saturated domain wall exists or not is a non-trivial dynamic question which can be answered only in a specific study of a particular theory in interest. This talk presents a brief review of our papers<sup>5-8</sup> where such a study has been performed.

The results concerning the BPS walls were obtained by solving numerically the first order BPS equations

$$\partial_z \phi = e^{i\delta} \partial \bar{\mathcal{W}} / \partial \bar{\phi}, \quad \partial_z \chi = e^{i\delta} \partial \bar{\mathcal{W}} / \partial \bar{\chi} \quad (13)$$

associated with the TVY lagrangian. The value of  $\delta$  to be chosen in Eq.(13) depends on the wall solution we are going to find. To fix it, note that the equations (13) admit an integral of motion:

$$\text{Im}[\mathcal{W}(\phi, \chi) e^{-i\delta}] = \text{const} \quad (14)$$

Indeed, we have

$$e^{-i\delta} \partial_z \mathcal{W} = e^{-i\delta} \left( \frac{\partial \mathcal{W}}{\partial \phi} \partial_z \phi + \frac{\partial \mathcal{W}}{\partial \chi} \partial_z \chi \right) = \left| \frac{\partial \mathcal{W}}{\partial \phi} \right|^2 + \left| \frac{\partial \mathcal{W}}{\partial \chi} \right|^2 = e^{i\delta} \partial_z \bar{\mathcal{W}}$$

The real wall connects the vacua with  $\mathcal{W} = 0$  and  $\mathcal{W} = -N/2(4m^{N-1}/3)^{1/N}$ . These boundary conditions are consistent with Eq.(14) only if  $e^{i\delta} = \pm 1$  (the sign depends on whether the walls goes from the symmetric vacuum to the asymmetric one when  $z$  goes from  $-\infty$  to  $+\infty$  or the other way round). For the complex walls, the boundary conditions and the conservation law (14) imply  $\delta = \frac{\pi}{N} \pm \frac{\pi}{2}$ .

To study the spectrum of the domain walls which are not BPS-saturated, one has to solve the equations of motion which are of the second order, and, technically, the problem is a little bit more involved.

## 2 Real Walls

The BPS equations (13) with the superpotential (6) and the kinetic term (7) have the form

$$\begin{aligned} \phi' &= e^{i\delta} \cdot 2\bar{\phi}^2 \ln\{\bar{\phi}^3 \bar{\chi}^{2(N-1)}\} \\ \chi' &= e^{i\delta} \cdot (N-1) \left[ \frac{4\bar{\phi}^3}{3\bar{\chi}} - m\bar{\chi} \right] \end{aligned} \quad (15)$$

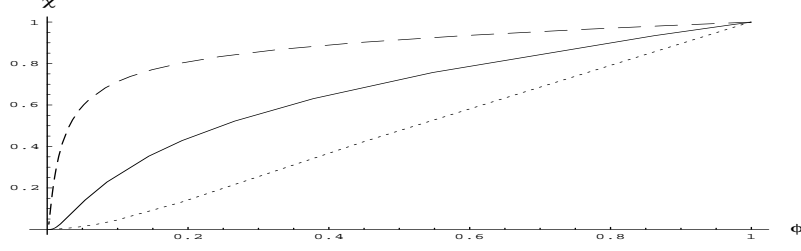


Figure 1: Real walls ( $N = 3$ ). The parametric plots for  $m = 1$  (solid line),  $m = .1$  (dashed line), and  $m = 10$  (dotted line).  $\phi$  and  $\chi$  are measured in units of  $R_*$  and  $\rho_*$ , respectively.

( $O' \equiv \partial_z O$ ). To find the wall interpolating between  $\phi = \chi = 0$  at  $z = -\infty$  and  $\phi = R_*$ ,  $\chi = \rho_*$  at  $z = \infty$ , we have to choose  $\delta = \pi$  (or  $\delta = 0$  for the wall going in the opposite direction). With this choice and the boundary conditions given, the solutions  $\phi(z)$  and  $\chi(z)$  are going to be real so that we have a simple system of just two first-order differential equations.

The dynamics of this system is essentially the same for any  $N$ . The solution exists for all masses. For large  $m$ , the heavy matter field can be integrated out, and we arrive at the BPS equation for the supersymmetric gluodynamics

$$\phi' = -2N\phi^2 \ln(\phi^3/R_*^3) \quad (16)$$

The solution of this equation with the boundary conditions  $\phi(-\infty) = 0$ ,  $\phi(\infty) = R_*$  can be expressed into integral logarithms.

An analytic solution of the system (15) can be found also for small masses. In the intermediate range of masses, the solution has to be found numerically. Parametric plots in the  $(\phi, \chi)$  plane for  $N = 3$  and different values of  $m$  are drawn in Fig. 1.

### 3 Domain Walls in Higgs Phase

The lagrangian (2) can be obtained from the full TVY lagrangian (6) in the limit of small masses if integrating out the heavy gauge *under the assumption* that the Higgs expectation value of the scalar matter fields is large. In this approach, chirally symmetric vacuum is not seen and there are only complex walls which turn out to be BPS saturated (we have seen, however, that the chirally symmetric vacuum and the real walls associated with it exist actually for all masses no matter how small they are). To find the profile of complex

walls in the Higgs phase, we have got to solve the BPS equations

$$\chi' = e^{-i\pi(N-2)/2N} \frac{\partial \bar{\mathcal{W}}}{\partial \bar{\chi}}, \quad (17)$$

where  $\mathcal{W}$  is the superpotential (2), with the boundary conditions

$$\chi(-\infty) = \rho_*; \quad \chi(\infty) = \rho_* e^{i\pi/N}; \quad (18)$$

It is convenient to introduce polar variables  $\chi = \rho e^{i\alpha}$ . The equations (17) acquire the form

$$\begin{aligned} \rho' &= (N-1) \left\{ m\rho \sin \gamma - \frac{4}{3\rho^{2N-1}} \sin[\gamma(N-1)] \right\} \\ \gamma' &= 2(N-1) \left\{ m \cos \gamma + \frac{4}{3\rho^{2N}} \cos[\gamma(N-1)] \right\} \end{aligned} \quad (19)$$

where  $\gamma \equiv 2\alpha - \pi/N$  changes from  $\gamma = -\pi/N$  at  $z = -\infty$  to  $\gamma = \pi/N$  at  $z = \infty$ . For  $N = 2$ , the solution is analytic:

$$\begin{aligned} \rho(z) &= \rho_* \\ \tan \gamma(z) &= \sinh[4m(z - z_0)] \end{aligned} \quad (20)$$

or in the complex form:

$$\chi(z) = \rho_* \frac{1 + ie^{4m(z-z_0)}}{\sqrt{1 + e^{8m(z-z_0)}}} \quad (21)$$

( $z_0$  is the position of the wall center). For  $N \geq 3$ , the solutions can be found numerically. The profiles for the ratio  $r(z) = \rho(z)/\rho_*$  in the interval  $z_0 \equiv 0 \leq z < \infty$  [it is a half of the wall, another half being restored by symmetry considerations:  $\rho(-z) = \rho(z)$ ] with different  $N = 3, 5, 10$  are presented in Fig. 2.

We see that the dependence  $\rho(z)$  is not flat anymore but displays a bump in the middle. To understand it, remind that the system (19) has the integral of motion (14). In our case, it amounts to

$$\frac{m(N-1)}{2} \rho^2 \cos \gamma - \frac{2}{3\rho^{2(N-1)}} \cos[\gamma(N-1)] = \frac{N}{2} \left( \frac{4m^{N-1}}{3} \right)^{1/N} \cos \frac{\pi}{N} \quad (22)$$

as follows from the boundary conditions (18) with  $\delta = \pi/N - \pi/2$ . In the middle of the wall,  $\gamma = 0$ , and the condition (22) implies

$$(N-1)x^2 - \frac{1}{x^{2(N-1)}} = N \cos \frac{\pi}{N} \quad (23)$$

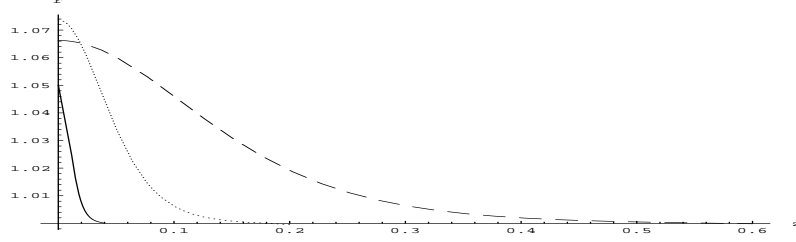


Figure 2: BPS walls in Higgs phase for  $N = 3$  (dashed line),  $N = 5$  (dotted line) and  $N = 10$  (solid line).

( $x \equiv r(0)$ ). It is not difficult to observe that the real root of the algebraic equation (23) is slightly greater than 1 for  $N \geq 3$ . When  $N$  is large,  $x - 1$  tends to zero  $\propto 1/N$ .

#### 4 Two BPS solutions and Phase Transition in Mass

When  $m \neq 0$ , the gauge degrees of freedom associated with the superfield  $\Phi$  do not decouple completely and should be taken into account. The full system (15) of the BPS equations for the complex domain walls has the form

$$\begin{aligned} \rho' &= (N-1) \left[ m\rho \sin(2\alpha - \pi/N) - \frac{4R^3}{3\rho} \sin(3\beta - \pi/N) \right] \\ \alpha' &= (N-1) \left[ m \cos(2\alpha - \pi/N) - \frac{4R^3}{3\rho^2} \cos(3\beta - \pi/N) \right] \\ R' &= -2R^2 \left[ \sin(3\beta - \pi/N) \ln(R^3 \rho^{2(N-1)}) + \cos(3\beta - \pi/N) [3\beta + 2\alpha(N-1)] \right] \\ \beta' &= 2R \left[ -\cos(3\beta - \pi/N) \ln(R^3 \rho^{2(N-1)}) + \sin(3\beta - \pi/N) [3\beta + 2\alpha(N-1)] \right] \end{aligned} \quad (24)$$

where, as in the previous section, we have chosen  $\delta = \pi/N - \pi/2$  and introduced the polar variables  $\chi = \rho e^{i\alpha}$ ,  $\phi = R e^{i\beta}$ . One should solve the system (24) with the boundary conditions

$$\begin{aligned} \rho(-\infty) &= \rho(\infty) = \rho_*; \quad R(-\infty) = R(\infty) = R_*; \\ \alpha(-\infty) &= \beta(-\infty) = 0; \quad \alpha(\infty) = \pi/N; \quad \beta(\infty) = -\frac{2(N-1)\pi}{3N} \end{aligned} \quad (25)$$

In the limit  $m \rightarrow 0$ , we can just freeze the heavy variables:

$$\beta = -2\alpha(N-1)/3; \quad R = \rho^{-2(N-1)/3} \quad (26)$$

in which case the first two equations in Eq.(24) reproduce the system (19) studied in the previous section. When mass is nonzero, but small enough, it is

possible to develop a systematic Born–Oppenheimer expansion and to find the profile of the wall as a series over the small parameter  $m$  (or rather  $m^{(2N+1)/3N}$  in our case). Not going in details<sup>7</sup>, we just present here for illustration how  $R(0)$ , the absolute value of the field  $\phi$  in the center of the wall, is changed with mass:

$$\begin{aligned} \eta(m) = \frac{R(0)}{R_0(0)} = 1 - \frac{(N-1)^2}{9R_0(0)} \left[ m + \frac{4}{3\rho_0^{2N}(0)} \right] - \\ \frac{(N-1)^3}{162R_0^2(0)} \left[ m + \frac{4}{3\rho_0^{2N}(0)} \right] \left[ m(7N-1) - \frac{32(N-1)}{3\rho_0^{2N}(0)} \right] + \\ O[m^3/R_0^3(0)] \end{aligned} \quad (27)$$

where  $R_0(0) \propto m^{(N-1)/(2N+1)}$  is related to  $\rho_0(0) = x\rho_*$  as in Eq.(26), and  $\rho_0(0)$  was found earlier when we studied the solutions of the reduced system in the Higgs phase.

When  $m$  is neither too large nor too small, the Born–Oppenheimer approximation does not apply and we are in a position to solve the full system of 4 equations (24) numerically. We did it for  $N = 2, 3, 4$ . The results turned out to be rather nontrivial and surprising. Namely, there turned out to be not one but *two* different BPS solutions. But they exist only for small enough masses; if the mass exceeds some critical value  $m_*$ , the BPS equation system has no solution at all. A kind of phase transition in mass occurs ! The values of the critical mass  $m_*$  have been found numerically:

$$m_*^{SU(2)} = 4.67059\dots, \quad m_*^{SU(3)} = .28604\dots, \quad m_*^{SU(4)} = 0.07539\dots \quad (28)$$

In Fig. 3, we plotted the dependence of  $\eta = R(0)/R_0(0)$  on  $m$  for both branches . We see that, at  $m = m_*$ , two branches are joined together. This *is* the reason why no solution exists at larger masses.

The upper BPS branch approaches the Higgs phase solution for the small masses. Speaking of the low branch, it approaches two widely separated real BPS walls for  $N = 2$  passing through the chirally symmetric vacuum in the middle, but for  $N \geq 3$  it presents a new nontrivial solution with the field values in the middle of the wall passing at some finite distance from the chirally symmetric vacuum even in the limit  $m \rightarrow 0$ <sup>7</sup>.

As is seen from Eq. (28), the value of  $m_*$  expressed in the units of  $\Lambda_{\text{SQCD}}$  drops rapidly with  $N$ . One can understand it looking at the Born–Oppenheimer result (27) Indeed, the critical mass  $m_*$  and the value of the mass where the Born–Oppenheimer expansion in Eq.(27) breaks down should be of the same order. For large  $N$ , the expansion parameter is  $\kappa \sim N^2(m/R_*) \sim$



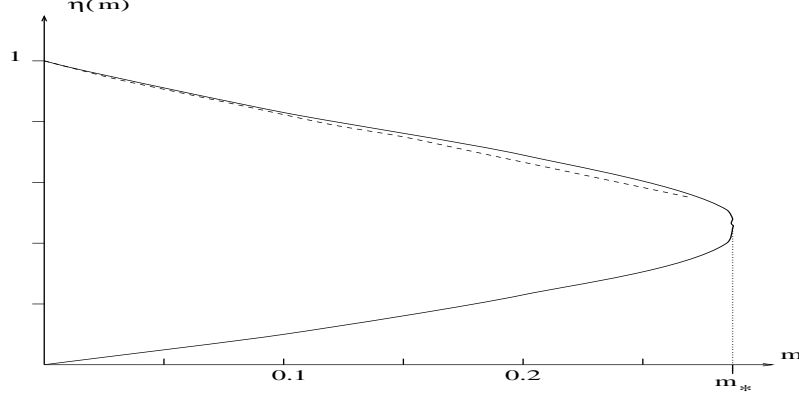


Figure 3: The ratio  $\eta = R(0)/R_0(0)$  as a function of mass for the  $SU(3)$  theory. The dashed line describes the analytic result (27) valid for small masses.

$N^2 m^{2/3}$ . Assuming  $\kappa \sim 1$ , we arrive at the conclusion that  $m_*$  falls down as

$$m_*(N) \propto N^{-3}$$

in the limit  $N \rightarrow \infty$ .

## 5 Solving equations of motion

Every solution of the BPS equations (13) is also a solution to the equations of motion, but not the other way round. It turns out that nontrivial non-BPS *complex* wall solutions exist. To find them, we have to solve the equations of motion for the potential (8) with the kinetic term  $|\partial\phi|^2 + |\partial\chi|^2$ . As earlier, it is convenient to introduce the polar variables  $\chi = \rho e^{i\alpha}$ ,  $\phi = R e^{i\beta}$  after which the equations of motion acquire the form

$$\begin{aligned} R'' - R\beta'^2 &= 8R^3[L(L+3/2) + \beta_+^2] + (N-1)^2 \left[ \frac{16R^5}{3\rho^2} - 4mR^2 \cos(\beta_-) \right] \\ R\beta'' + 2R'\beta' &= 12R^3\beta_+ + 4(N-1)^2 mR^2 \sin(\beta_-) \\ \rho'' - \rho\alpha'^2 &= (N-1) \frac{8R^4}{\rho} L + (N-1)^2 \left( m^2 \rho - \frac{16R^6}{9\rho^3} \right) \\ \rho\alpha'' + 2\rho'\alpha' &= (N-1) \frac{8R^4}{\rho} \beta_+ - (N-1)^2 \frac{8mR^3}{3\rho} \sin(\beta_-) , \end{aligned} \quad (29)$$

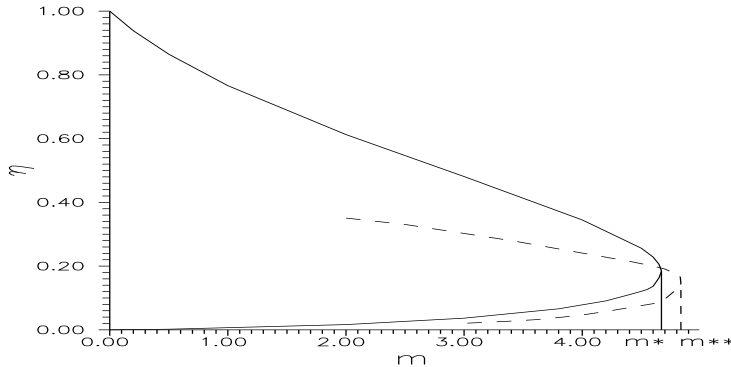


Figure 4: The ratio  $\eta = R(0)/R_0(0)$  for the solutions of the equations of motion as a function of mass for the  $SU(2)$  theory. The solid lines describe the BPS solutions and the dashed lines describe the non-BPS wall and the sphalerons.

where  $L = \ln[R^3 \rho^{2(N-1)}]$ ,  $\beta_+ = 3\beta + 2(N-1)\alpha$ ,  $\beta_- = 3\beta - 2\alpha$ . The boundary conditions (25) are assumed.

The phase space of the system (29) is 8-dimensional and the boundary problem (which we solved by shooting method) is somewhat more tricky than for the BPS case. In particular, the trajectories become more and more unstable as  $N$  grows. Finding the trajectory going from one vacuum to another is something like lancing the ball to roll along a razorblade mountain ridge from one top to another. Our computer managed to do it for  $N = 2$  and  $N = 3$ .

All the solutions obtained are presented in Fig. 4 ( $N = 2$ ) and in Fig. 5 ( $N = 3$ ) where the parameter  $R(0)$  is plotted as a function of mass [we normalized  $R(0)$  at its value  $R_0(0) = R_*$  ( $N = 2$ ) and  $R_0(0) = .918 \dots R_*$  ( $N = 3$ ) for the upper BPS branch in the limit  $m \rightarrow 0$ ]. For small masses, there are several solutions. We obtain first of all the BPS solutions studied before (solid lines in Figs. 4, 5). We find also two new solution branches drawn with the dashed lines. We see that, similarly to the BPS branches, two new dashed branches fuse together at some value  $m = m_{**} > m_*$ . No solution for the system (29) exist at  $m > m_{**}$ .

We see that the pattern of the solutions for  $N = 2$  and  $N = 3$  is qualitatively similar. To understand it, assume first that  $m < m_*$  and draw the energy functional  $E$  for field configurations with wall boundary conditions minimized over all parameters except the value of  $R(0)$  which is kept fixed (see Fig. 6a). For very small  $R(0)$ , our configuration nearly passes the chirally symmetric minimum and the minimum of the energy corresponds to two widely separated real walls. Thus  $E[R(0) = 0] = 2\epsilon_r$  with  $\epsilon_r$  given in Eq.(11). Two minima in

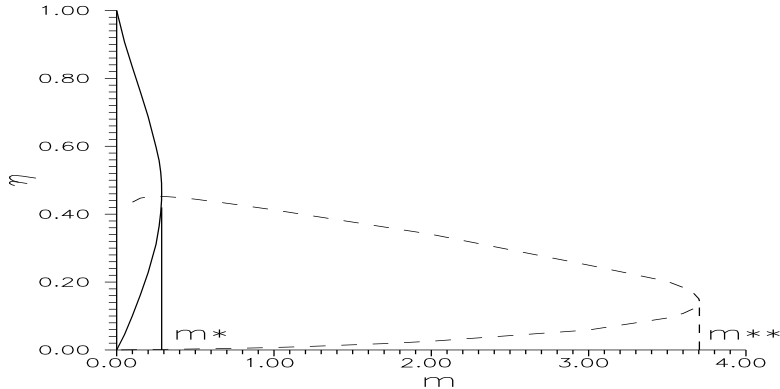


Figure 5: The same for  $N = 3$ .

Fig. 6a correspond to BPS solutions with the energy  $\epsilon_c$ . They are separated by an energy barrier (for illustrative purposes, the height of the barriers is exaggerated). The top of this barrier (actually, this is a saddle point with only one unstable mode corresponding to  $R(0)$ , in other words — a *sphaleron*) is a solution described by the upper dashed line in Figs. 4, 5. The lower dashed line corresponds to the local maximum on the energy barrier separating the lower BPS branch and the configuration of two distant real walls at  $R(0) = 0$ .<sup>b</sup>

At  $m = m_*$ , two BPS minima fuse together and the energy barrier separating them disappears. The upper sphaleron branch coincides with the BPS solution at this point. When  $m$  is increased above  $m_*$ , the former BPS minimum is still a minimum of the energy functional, but its energy is now above the BPS bound (see Fig.6b). The corresponding solution is described by the analytic continuation of the upper sphaleron branch. The lower dashed branch in the region  $m_* < m < m_{**}$  is still a sphaleron. At the second critical point  $m = m_{**}$ , the picture is changed again (see Fig.6c). The local maximum and the local minimum fuse together and the only one remaining stationary point does not correspond to an extremum of the energy functional anymore. At larger masses, no non-trivial stationary points are left.

There is one distinction, however. For  $N = 2$ , the second critical mass

<sup>b</sup>For  $N = 3$ , in contrast to the case  $N = 2$ , the existence of such a barrier could not be established from the BPS spectrum alone. The matter is that, while  $2\epsilon_r = \epsilon_c$  for  $N = 2$  and the presence of the maximum is guaranteed by the Roll theorem,  $2\epsilon_r > \epsilon_c$  for  $N = 3$ , and one could in principle imagine a situation where  $E$  falls down monotonically when  $R(0)$  is increased from zero up to its value at the lower BPS branch. Our numerical results strongly suggest, however, that the energy barrier (though a tiny one) is present.

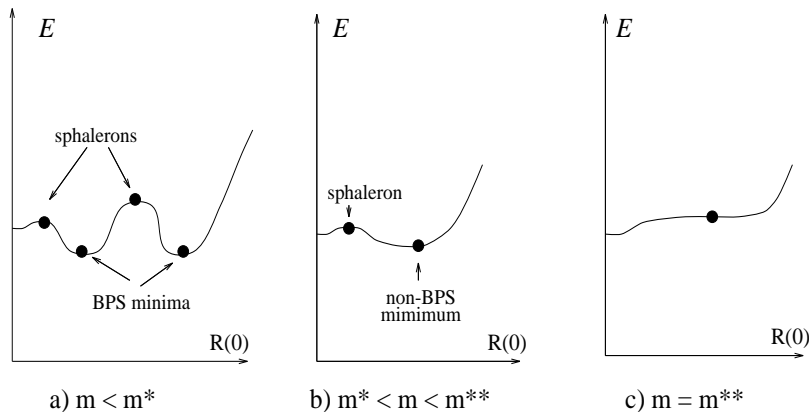


Figure 6: Illustrative profiles of the energy functional vs.  $R(0)$ .

$m_{**} \approx 4.83$  is very close to  $m_*$  and the energy of the non-BPS wall at  $m = m_{**}$  deviates from the BPS limit by less than  $10^{-5}$  ! When  $N = 3$ ,  $m_{**} \approx 3.704$  differs essentially from  $m_*$  and the energy of the wall at  $m = m_{**}$ , being very close to the energy of two widely separated real walls  $2\epsilon_r$ , differs from the BPS limit  $\epsilon_c$  for the complex walls. One can speculate that, while  $m_*$  drops rapidly as  $N$  grows, the value of  $m_{**}$  is roughly constant in the large  $N$  limit. To be precise, we did not perform a careful numerical study for  $N > 3$  and cannot therefore exclude the possibility that, for large enough  $N$ , the second critical mass disappears altogether and the non-BPS complex wall solutions exist for any mass. Our bet, however, is that it does not happen.

## 6 Discussion.

Our main result is that, while the real BPS domain walls connecting the chirally symmetric and a chirally asymmetric vacua are present at all masses, the complex BPS walls interpolating between different asymmetric vacua exist only for small enough masses  $m < m_*$ ,  $m_*$  being given in Eq.(28). A kind of phase transition associated with the restructuring of the wall spectrum occurs.<sup>c</sup>

Furthermore, also a second critical mass  $m_{**}$  exists beyond which no complex wall solution can be found whatsoever. That means in particular that

<sup>c</sup>Needless to say, it is not a phase transition of a habitual thermodynamic variety. In particular, the vacuum energy is zero both below and above the phase transition point — supersymmetry is never broken here. Hence  $E_{vac}(m) \equiv 0$  is not singular at  $m = m_*$ .

no domain walls connecting different chirally asymmetric vacua are left in the pure supersymmetric Yang–Mills theory corresponding to the limit  $m \rightarrow \infty$ , and only the real domain walls connecting the chirally symmetric and a chirally asymmetric vacuum states survive in this limit. Note that that contradicts a recent *assumption* by Witten<sup>9</sup> that it is complex rather than real domain walls which are present in the pure SYM theory (Witten discussed them in the context of brane dynamics).

One has to make a reservation here: our result was obtained in the framework of the TVY effective lagrangian (6) whose status [in contrast to that of the lagrangian (2)] is not absolutely clear: the field  $\Phi$  describes heavy degrees of freedom (viz. a scalar glueball and its superpartner) which are not nicely separated from all the rest. However, the form of the superpotential (6) and hence the form of the lagrangian for static field configurations is *rigidly* dictated by symmetry considerations; the uncertainty involves only kinetic terms. It is reasonable to assume that, as far as the vacuum structure of the theory is concerned (but not e.g. the excitation spectrum — see Ref.<sup>8</sup> for detailed discussion), the effective TVY potential (6) can be trusted. A recent argument against using Eq. (6) that the chirally symmetric phase whose existence follows from the TVY lagrangian does not fulfill certain discrete anomaly matching conditions<sup>10</sup> is probably not sufficient. First, it assumes that the excitation spectrum in the symmetric phase is the same as it appears in the TVY lagrangian which is not justified. Second, it was argued recently that the TVY lagrangian describes actually *all* the relevant symmetries of the underlying theory and the absence of the anomaly matching is in a sense an “optical illusion”<sup>11</sup>.

It would be very interesting to repeat the numerical study performed here for the effective lagrangian with the same TVY superpotential (6), but a different kinetic term. Probably, it makes sense to start with the VY lagrangian for the pure SYM theory and try tentatively for example

$$\mathcal{L}'_{\text{kin}} = \int d^4\theta \frac{\bar{\Phi} D^2 \Phi}{(\bar{\Phi} \Phi)^{1/2}} \quad (30)$$

(One *cannot* write instead a general Kähler term  $\int d^4\theta F(\bar{\Phi}, \Phi)$ . It would involve a dimensionful scale and would spoil the anomaly matching condition  $\partial \mathcal{L}_{\text{eff}} / \partial (\ln \Lambda) \sim G^2$ ). Our *guess* is that, for the VY lagrangian with the kinetic term (30), the real walls talking to the chirally symmetric vacuum would also be present and the complex walls would be also absent. For a generalized TVY lagrangian, the particular values of  $m_*$  and  $m_{**}$  would be different, but the qualitative pictures in Figs. 4, 5 would not change.

## Acknowledgments

This work was supported in part by the RFBR–INTAS grants 93–0283, 94–2851, 95–0681, and 96–370, by the RFFI grants 96–02–17230, 97–02–17491, and 97–02–16131, by the RFBR–DRF grant 96–02–00088, by the U.S. Civilian Research and Development Foundation under award # RP2–132, and by the Schweizerischer National Fonds grant # 7SUPJ048716.

## References

1. V. Novikov, M. Shifman, A. Vainshtein, and V. Zakharov, *Nucl. Phys. B* **229**, 407 (1983); *Phys. Lett. B* **166**, 334 (1986); I. Affleck, M. Dine, and N. Seiberg, *Nucl. Phys. B* **241**, 493 (1984) 493; *Nucl. Phys. B* **256**, 557 (1985); G. Rossi and G. Veneziano, *Phys. Lett. B* **138**, 195 (1984); D. Amati, K. Konishi, Y. Meurice, G. Rossi, and G. Veneziano, *Phys. Rep.* **162**, 557 (1988); M. Shifman, *Int. J. Mod. Phys. A* **11**, 5761 (1996).
2. A. Kovner and M. Shifman, *Phys. Rev. D* **56**, 3296 (1997).
3. T. Taylor, G. Veneziano, and S. Yankielowicz, *Nucl. Phys. B* **218**, 493 (1983).
4. G. Dvali and M. Shifman, *Phys. Lett. B* **396**, 64 (1997); B. Chibisov and M. Shifman, *Phys. Rev. D* **56**, 7990 (1997).
5. A. Kovner, M. Shifman, and A. Smilga, *Phys. Rev. D* **56**, 7978 (1997).
6. A. Smilga and A. Veselov, *Phys. Rev. Lett.* **79**, 4529 (1997); *Phys. Lett. B* **428**, 303 (1998).
7. A. Smilga, hep-th/9711032, *Phys. Rev. D*, to appear.
8. A. Smilga and A. Veselov, *Nucl. Phys. B* **515**, 163 (1998).
9. E. Witten, *Nucl. Phys. B* **507**, 658 (1997).
10. C. Csaki and H. Murayama, *Nucl. Phys. B* **515**, 114 (1998).
11. I. Kogan, A. Kovner, and M. Shifman, *Phys. Rev. D* **57**, 5195 (1998).